

## Triisopropyltriazacyclononane Copper(II): An Efficient Phosphodiester Hydrolysis Catalyst and DNA Cleavage Agent

Kathryn M. Deck, T. Andrew Tseng, and Judith N. Burstyn\*<sup>†</sup>

Department of Chemistry, University of Wisconsin—Madison, Madison, Wisconsin 53706

Received July 2, 2001

A 6000-fold rate enhancement has been observed for the hydrolysis of bis(*p*-nitrophenyl)phosphate (BNPP) in the presence of 0.2 mM Cu(*i*-Pr<sub>3</sub>[9]aneN<sub>3</sub>)<sup>2+</sup> at pH 9.2 and 50 °C. In a direct comparison, the rate of hydrolysis of BNPP is accelerated at least 60-fold over the previously reported catalyst Cu([9]aneN<sub>3</sub>)<sup>2+</sup>. As observed for Cu([9]aneN<sub>3</sub>)<sup>2+</sup>, hydrolysis is selective for diesters over monoesters. Hydrolysis of BNPP by Cu(*i*-Pr<sub>3</sub>[9]aneN<sub>3</sub>)<sup>2+</sup> is catalytic, exhibiting both rate enhancement and turnover. The reaction is inhibited by both *p*-nitrophenyl phosphate and inorganic phosphate. The reaction is first-order in substrate and half-order in metal complex, with a *k*<sub>1.5</sub> of 0.060 ± 0.004 M<sup>-1/2</sup> s<sup>-1</sup> at 50 °C. The temperature dependence of the rate constant results in a calculated activation enthalpy ( $\Delta H^\ddagger$ ) of 51 ± 2 kJ mol<sup>-1</sup> and activation entropy ( $\Delta S^\ddagger$ ) of -110 ± 6 J mol<sup>-1</sup> K<sup>-1</sup>. The kinetic *pK*<sub>a</sub> of 7.8 ± 0.2 is close to the thermodynamic *pK*<sub>a</sub> of 7.9 ± 0.2, consistent with deprotonation of a coordinated water molecule in the active form of the catalyst. The active catalyst [Cu(*i*-Pr<sub>3</sub>[9]aneN<sub>3</sub>)(OH)(OH<sub>2</sub>)]<sup>+</sup> is in equilibrium with an inactive dimer, and the formation constant for this dimer is between 216 and 1394 M<sup>-1</sup> at pH 9.2 and 50 °C. Temperature dependence of the dimer formation constant *K*<sub>f</sub> indicates an endothermic enthalpy of formation for the dimer of 27 ± 3 kJ mol<sup>-1</sup>. The time course of anaerobic DNA cleavage by Cu(*i*-Pr<sub>3</sub>[9]aneN<sub>3</sub>)<sup>2+</sup> is presented over a wide range of concentrations at pH 7.8 at 50 °C. The concentration dependence of DNA cleavage by Cu([9]aneN<sub>3</sub>)<sup>2+</sup> and Cu(*i*-Pr<sub>3</sub>[9]aneN<sub>3</sub>)<sup>2+</sup> reveals a maximum cleavage efficiency at sub-micromolar concentrations of cleavage agent. DNA cleavage by Cu(*i*-Pr<sub>3</sub>[9]aneN<sub>3</sub>)<sup>2+</sup> is twice as efficient at pH 7.8 as at pH 7.2.

### Introduction

Although many metallonucleases exist that rapidly hydrolyze DNA at neutral pH and physiological temperatures, it has proven more challenging to synthesize small-molecule catalysts capable of similar chemistry. Such inexpensive catalysts would potentially be valuable tools in biotechnology, facilitating the manipulation of DNA in a variety of applications. Because of the challenges inherent in identifying the products of DNA cleavage reactions, it is common to use small-molecule phosphodiester models as tools in the development of new catalysts. Transition metal ions<sup>1</sup> and complexes,<sup>2–5</sup> lanthanide ions<sup>6–8</sup> and complexes,<sup>9–12</sup> and

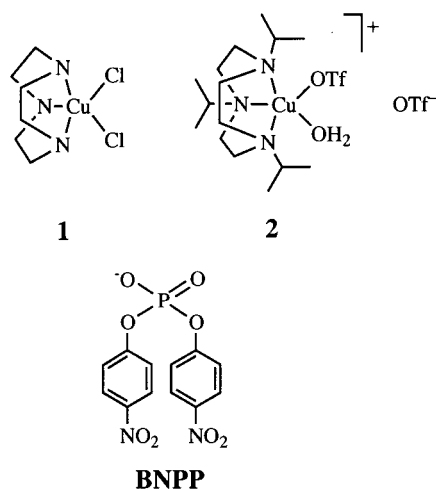
actinides<sup>13,14</sup> have all been utilized as catalysts for the hydrolysis of DNA and model phosphodiester. Although lanthanides have proven effective in DNA cleavage, the mechanism of the reaction has been difficult to elucidate. The identification of metal complexes that are effective at cleaving DNA and suitable for mechanistic study remains a challenge, but such complexes are essential in order that a thorough understanding of the chemistry may be obtained.

<sup>†</sup> E-mail: burstyn@chem.wisc.edu.

- (1) Moss, R. A.; Zhang, J.; Ragunathan, K. G. *Tetrahedron Lett.* **1998**, 39, 1529–1532.
- (2) Hegg, E. L.; Burstyn, J. N. *Coord. Chem. Rev.* **1998**, 173, 133–165.
- (3) Molenveld, P.; Engbersen, J. F. J.; Reinhoudt, D. N. *Chem. Soc. Rev.* **2000**, 29, 75–86.
- (4) Williams, N. H.; Cheung, W.; Chin, J. J. *Am. Chem. Soc.* **1998**, 120, 8079–8087.
- (5) Williams, N. H.; Lebuis, A.-M.; Chin, J. J. *Am. Chem. Soc.* **1999**, 121, 3341–3348.

- (6) Komiyama, M.; Sumaoka, J. *Curr. Opin. Chem. Biol.* **1998**, 2, 751–757.
- (7) Gómez-Tagle, P.; Yatsimirsky, A. K. *J. Chem. Soc., Dalton Trans.* **1998**, 2957–2979.
- (8) Roigk, A.; Schneider, H.-J. *Eur. J. Org. Chem.* **2001**, 205–209.
- (9) Franklin, S. J. *Curr. Opin. Chem. Biol.* **2001**, 5, 201–208.
- (10) Branun, M. E.; Tipton, A. K.; Zhu, S.; Que, L., Jr. *J. Am. Chem. Soc.* **2001**, 123, 1898–1904.
- (11) Jurek, P. E.; Jurek, A. M.; Martell, A. E. *Inorg. Chem.* **2000**, 39, 1016–1020.
- (12) Ragunathan, K. G.; Schneider, H.-J. *Angew. Chem., Int. Ed. Engl.* **1996**, 35, 1219–1221.
- (13) Moss, R. A.; Bracken, K.; Zhang, J. *Chem. Commun.* **1997**, 563–564.
- (14) Moss, R. A.; Zhang, J.; Bracken, K. *Chem. Commun.* **1997**, 1639–1640.

Chart 1



Complexes of copper(II) are known to be effective DNA cleavage agents and hydrolysis catalysts, and these complexes are structurally well-characterized and suitable for mechanistic studies. A wide range of ligand environments for copper(II) have proven effective in DNA and phosphodiester hydrolysis; recent examples include simple macrocycles,<sup>15,16</sup> amino acid residues,<sup>17</sup> and complex polysaccharides.<sup>18,19</sup> We have chosen a well-characterized macrocyclic ligand environment for copper(II), studying the reactivity of the copper(II) macrocycles with model phosphodiester substrates, for which detailed mechanistic studies can be carried out, in parallel with DNA cleavage studies.

In prior studies we determined the mechanism of hydrolysis of bis(*p*-nitrophenyl)phosphate (BNPP) by the triazaclononane copper(II) cation (**1**, Chart 1).<sup>20–22</sup> Important structural features of complex **1** include a labile metal cation and two cis-oriented accessible coordination sites. The activity of **1** was limited by a monomer–dimer equilibrium, which greatly favored the dimeric, inactive form of the complex.<sup>21</sup> Subsequent studies revealed that **1** cleaves DNA at pH 7.8 under anaerobic conditions, suggesting that a hydrolytic mechanism might be operative.<sup>23</sup> In addition, **1** hydrolyzes RNA,<sup>24</sup> peptides and proteins.<sup>25</sup> Structure–activity studies on copper(II) complexes with larger macrocycles revealed that greater hydrolytic reactivity correlated with a decrease in the dimerization constant.<sup>26</sup> Preliminary

studies showed that the *N*-alkylated copper macrocycle [Cu(*i*-Pr<sub>3</sub>[9]aneN<sub>3</sub>)(OTf)(OH<sub>2</sub>)]OTf (**2**) was more effective than **1** in promoting DNA cleavage.<sup>23</sup> In this paper we report the kinetics of BNPP hydrolysis by **2**, including a quantitative comparison of **2** with the family of triaza macrocyclic complexes previously studied, and more detailed studies of DNA cleavage by both **1** and **2**.

## Experimental Section

**Reagents.** Sodium bis(*p*-nitrophenyl)phosphate, disodium 4-nitrophenyl phosphate, tetrasodium pyrophosphate, EDTA, ampicillin, type III-A agarose, and the buffers 2-[*N*-morpholino]ethanesulfonic acid (MES), *N*-[2-hydroxyethyl]piperazine-*N'*-[2-ethanesulfonic acid] (HEPES), and *N*-[2-hydroxyethyl]piperazine-*N'*-[2-propanesulfonic acid] (HEPPSO) were purchased from Sigma Chemical Co. The buffer 2-[*N*-cyclohexylamino]ethanesulfonic acid (CHES) was purchased from Fluka. Water was purified by passage through a Millipore purification system to a resistance of 18 MΩ and sterilized by autoclave. Reaction solutions for DNA cleavage were prepared according to standard sterile techniques. All other chemicals were purchased from Aldrich and used without further purification.

The metal complex Cu([9]aneN<sub>3</sub>)Cl<sub>2</sub> (**1**) was synthesized as previously described.<sup>21</sup> [Cu(*i*-Pr<sub>3</sub>[9]aneN<sub>3</sub>)(OTf)(OH<sub>2</sub>)](OTf) (**2**) was synthesized according to the literature procedure<sup>27</sup> or was provided as a gift from Professor William Tolman (University of Minnesota).

**Instrumentation.** Kinetic measurements were performed using Varian Cary 4 Bio UV/vis spectrophotometer equipped with a Cary thermostated multicell block and Peltier temperature controller. For pH determinations, an Orion Research digital ion analyzer model 611 equipped with a Ross semi-micro temperature compensation electrode was utilized and the temperature was regulated by a circulating water bath (Lauda MT). Ethidium-stained agarose gels were imaged on a Molecular Dynamics FluorImager 575 equipped with a 610 nm long pass filter.

**Kinetics of BNPP Hydrolysis.** Hydrolysis of BNPP produces 4-nitrophenolate with a wavelength of maximum absorbance at 400 nm and an extinction coefficient of 18 700 L mol<sup>-1</sup> cm<sup>-1</sup>. The initial rate of production of 4-nitrophenolate was monitored spectrophotometrically at 400 nm, and the concentration of 4-nitrophenolate produced was calculated from the extinction coefficient. Reactions performed at pH < 9 were corrected for the degree of ionization of the 4-nitrophenol product at the reaction temperature and pH.<sup>28</sup> To correct for the spontaneous hydrolysis of the phosphodiester, the rate of each reaction was measured against a reference cell, which was identical in composition except lacking the metal complex. Spontaneous hydrolysis was minimal across the pH range studied (5–9.5). The reaction was monitored for less than 5% conversion of substrate to products. The initial rate of reaction was obtained directly from a plot of 4-nitrophenolate concentration versus time, which was linear with *R* > 0.997. Reactions were performed in glass cells sealed with Teflon-lined screw caps and were maintained at pH 9.2 with 50.0 mM CHES buffer and an ionic strength of 0.10 M maintained with NaNO<sub>3</sub>, unless otherwise

- (15) Itoh, T.; Hisada, H.; Usui, Y.; Fujii, Y. *Inorg. Chim. Acta* **1998**, *283*, 51–60.  
 (16) Wall, M.; Linkletter, B.; Williams, D.; Lebus, A.-M.; Hynes, R. C.; Chin, J. *J. Am. Chem. Soc.* **1999**, *121*, 4710–4711.  
 (17) Ren, R.; Yang, P.; Zheng, W.; Hua, Z. *Inorg. Chem.* **2000**, *39*, 5454–5463.  
 (18) Sreedhara, A.; Freed, J. D.; Cowan, J. A. *J. Am. Chem. Soc.* **2000**, *122*, 8814–8824.  
 (19) Molenveld, P.; Engbersen, J. F. J.; Kooijman, H.; Spek, A. L.; Reinhoudt, D. N. *J. Am. Chem. Soc.* **1998**, *120*, 6726–6737.  
 (20) Burstyn, J. N.; Deal, K. A. *Inorg. Chem.* **1993**, *32*, 3585–3586.  
 (21) Deal, K. A.; Burstyn, J. N. *Inorg. Chem.* **1996**, *35*, 2792–2798.  
 (22) Deal, K. A.; Hengge, A. C.; Burstyn, J. N. *J. Am. Chem. Soc.* **1996**, *118*, 1713–1718.  
 (23) Hegg, E. L.; Burstyn, J. N. *Inorg. Chem.* **1996**, *35*, 7474–7481.  
 (24) Hegg, E. L.; Deal, K. A.; Kiessling, L. L.; Burstyn, J. N. *Inorg. Chem.* **1997**, *36*, 1715–1718.  
 (25) Hegg, E. L.; Burstyn, J. N. *J. Am. Chem. Soc.* **1995**, *117*, 7015–7016.

- (26) Hegg, E. L.; Mortimore, S.; Cheung, C.-L.; Huyett, J. E.; Burstyn, J. N. *Inorg. Chem.* **1999**, *38*, 2961–2968.  
 (27) Halfen, J. A.; Mahapatra, S.; Wilkinson, E. C.; Gengenbach, A. J.; Young, V. G., Jr.; Que, L., Jr.; Tolman, W. B. *J. Am. Chem. Soc.* **1996**, *118*, 763–776.  
 (28) Martell, A. E.; Smith, R. M. *Critical Stability Constants*; Plenum Press: New York, 1977.

stated. Both sample and reference cells were equilibrated for 5 min at 50 °C before the reaction was begun. Reactions were initiated by the addition of either substrate or metal complex. Rate enhancement was measured directly from the rate of hydrolysis of 1.0 mM BNPP in 50.0 mM CHES, pH 9.24 ± 0.05, 0.10 M ionic strength at 50 °C in both the presence and absence of 0.20 mM **2**, referenced against water. Substrate selectivity was studied by comparing the rates of BNPP and 4-nitrophenyl phosphate hydrolysis in the presence of 0.20 mM **2**. The reactions were 1.0 mM in substrate. Temperature dependence of the rate constant of BNPP hydrolysis was studied at 15, 28, 35, and 50 °C with varying concentrations of **2**, and the reactions were initiated by the addition of BNPP (1.0 mM). Ionic strength dependence was studied using reactions of 0.80 mM BNPP with 0.30 mM Cu(*i*-Pr<sub>3</sub>[9]aneN<sub>3</sub>)<sup>2+</sup> at both pH 7.13 ± 0.02 (50.0 mM HEPES) and pH 9.14 ± 0.04 (50.0 mM CHES). The ionic strength was adjusted with NaNO<sub>3</sub> and was varied from 50 to 450 mM. Details of inhibition, metal dependence, substrate dependence, and pH dependence experiments are provided in the figure legends.

**Product Analysis for BNPP Hydrolysis.** For product analysis, a 3.00 mL reaction consisting of 1.0 mM **2**, 50.0 mM HEPES (pH 7.8), and 2.0 mM BNPP was prepared. The solution was incubated at 50 °C, and samples were withdrawn after 0 min, 8 min, 15 min, 1.5 h, and 2 h and applied to polyethylene imine (PEI) cellulose F TLC plates (EM Science). Elution with 0.1 M LiCl gave a chromatogram consistent with the expected products nitrophenyl phosphate and *p*-nitrophenolate. No other products were observed.

**Turnover.** Turnover was demonstrated by preparing a reaction mixture consisting of 0.10 mM **2**, 5.0 mM BNPP, and 50.0 mM CHES (pH 9.2), at 0.10 M ionic strength adjusted with NaNO<sub>3</sub>. To correct for background hydrolysis, the reference reaction was identical in all respects except that it contained no metal complex. The solutions were incubated at 50 °C, and the reaction was monitored by periodically withdrawing aliquots, diluting both sample and reference, and measuring absorbance at 400 nm by direct difference. The dilution was necessary to bring the absorbance onto a measurable scale. The concentration of product in the reaction vial was then calculated. The experiment was run in triplicate.

**pH Titration.** Solutions of **2** were prepared at concentrations between 0.5 and 2.7 mM with ionic strength adjusted to 0.10 M using NaNO<sub>3</sub>. The solutions were titrated with both acid (0.1 M HCl) and base (0.05 M NaOH), with stirring, over a pH range of 4–12. Titrations were performed at room temperature in air and at 50 °C under nitrogen. The value reported for each set of conditions represents the average of at least two titrations. The pH meter was calibrated using commercial pH standards immediately prior to each titration.

**DNA Cleavage Studies.** The supercoiled plasmid, pBluescript II ks(–) was purchased from Stratagene Cloning Systems. The DNA was transformed into DH5α bacterial cells via electroporation, and the transformed bacteria were cultured in medium containing ampicillin. The supercoiled DNA was harvested according to standard procedures<sup>29</sup> and purified using the Plasmid Mega Kit purification system from Qiagen. All DNA cleavage reactions were performed anaerobically. Solutions were prepared in a nitrogen-filled glovebag in microfuge tubes with O-ring sealed caps. Deoxygenated water and HEPPSO and HEPES buffers were prepared by vacuum filtration through 0.22 μm cellulose acetate filtration units from Corning. The deoxygenated water and buffers were stored under an argon atmosphere prior to use. Solutions (50

**Table 1.** BNPP Hydrolysis by **1** and **2**: Direct Rate Comparison<sup>a</sup>

copper complex	initial rate (10 <sup>–8</sup> M s <sup>–1</sup> )	
	pH 7.2	pH 9.2
<b>1</b>	0.060 ± 0.006	0.21 ± 0.01
<b>2</b>	4.28 ± 0.09	11.7 ± 0.7

<sup>a</sup> Reaction conditions: 0.20 mM metal complex, 1.0 mM BNPP, pH 7.2 (50 mM HEPES) or pH 9.2 (50 mM CHES), 0.10 M ionic strength maintained with NaNO<sub>3</sub>, 50 °C.

μL total volume) containing 0.05 mg/mL pBluescript II ks(–) supercoiled DNA (25 nM in supercoiled DNA or 150 μM in phosphate units) were incubated in sterile 0.5 mL microfuge tubes with varying concentrations of [Cu(*i*-Pr<sub>3</sub>[9]aneN<sub>3</sub>)(OTf)(OH<sub>2</sub>)](OTf) at 50 °C. The pH was maintained at 7.8 or 7.2 with 40 mM HEPPSO, as indicated. The reaction tubes were transferred to an argon-filled vacuum desiccator and incubated in the sealed desiccator at 50 °C. The reactions were quenched by cooling to 0 °C; bromophenol blue and xylene cyanol were added to each reaction tube, and if necessary, the tubes were stored at –20 °C until analyzed by agarose gel electrophoresis. (As a check of the quenching conditions, duplicate reactions were run in parallel where the reactions were quenched via ethanol precipitation instead of freezing; the results showed no difference in the amount of plasmid cleavage.)

**Product Analysis and Quantitation for DNA Cleavage Reactions.** The extent of supercoiled DNA cleavage was determined via densitometric analysis of ethidium bromide-containing agarose gels. Plasmid cleavage products were separated on an ethidium bromide-containing agarose gel (0.8%) in 0.5 × TBE buffer for 2.5 h at 130 V. The amount of cleavage was determined by fluorescence imaging and analysis with the program ImageQuaNT version 4.1 using the volume quantitation method. In all cases, background fluorescence was determined by reference to a lane containing no DNA. A correction factor of 1.42 was utilized to account for the decreased ability of ethidium bromide to intercalate into supercoiled DNA (form I) versus nicked DNA (form II) and linear DNA (form III).<sup>30</sup> The relative amounts of the different forms of DNA were determined by dividing the fluorescence intensity of each band by the sum of fluorescence intensities for all bands in that lane. The total percent of DNA cleaved was calculated as {total % cleaved = [(% form II) + 2(% form III)]} since there must be at least two cleavage events to go from supercoiled to linear DNA.<sup>23</sup> All experiments were performed at least in triplicate. The error bars in the graphs denote standard deviations that were determined by using the formula for a small number of data points.

## Results

**Catalytic Efficiency of Cu(*i*-Pr<sub>3</sub>[9]aneN<sub>3</sub>)<sup>2+</sup>.** The efficiency and catalytic properties of [Cu(*i*-Pr<sub>3</sub>[9]aneN<sub>3</sub>)(OTf)(OH<sub>2</sub>)]OTf (**2**) were studied with respect to BNPP hydrolysis. Direct comparison between **2** and the parent complex Cu([9]aneN<sub>3</sub>)Cl<sub>2</sub> (**1**) revealed that the triisopropyl derivative is considerably more efficient in promoting hydrolysis of BNPP (Table 1). At pH 7.2, the increase in rate was 70-fold, while, at pH 9.2, the increase was 60-fold. Rate enhancement and turnover studies demonstrated that BNPP hydrolysis is catalytic for the triisopropyl derivative, as it is for the parent complex.<sup>20</sup> The rate of the metal-catalyzed reaction is 6000

(29) Sambrook, J.; Fritsch, E. F.; Maniatis, T. In *Molecular Cloning*, 2nd ed.; Ford, N., Ed.; Cold Spring Harbor Laboratory: New York, 1989.

(30) Haidle, C. W.; Lloyd, R. S.; Robberson, D. L. In *Bleomycin: Chemical, Biochemical, and Biological Aspects*; Hecht, S. M., Ed.; Springer-Verlag: New York, 1979; pp 222–243.

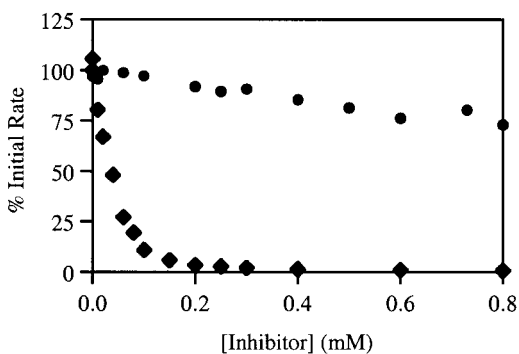


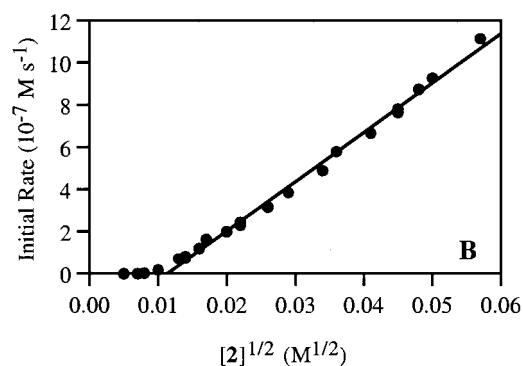
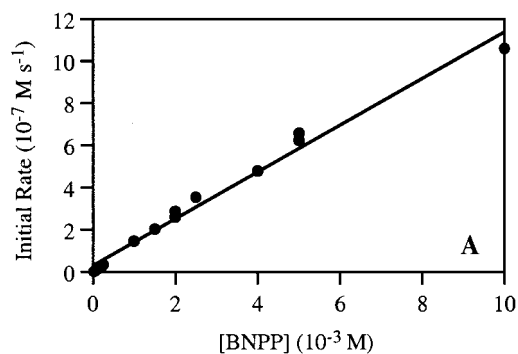
**Figure 1.** Inhibition of **2**-mediated BNPP hydrolysis. Reactions were carried out at pH 9.2 in 50 mM CHES buffer, at an ionic strength of 0.10 M (adjusted with NaNO<sub>3</sub>). [**2**] was 0.20 mM, and [BNPP] was 0.60 mM. Inhibitors were nitrophenyl phosphate ● (0.01–0.8 mM) and sodium pyrophosphate ◆ (0.02–0.8 mM).

times greater than the rate of the hydroxide-catalyzed reaction at the same pH (9.2). Larger than stoichiometric amounts of product are produced, with 7 turnovers of the catalyst being observed over a 2 week period. The hydrolysis of BNPP by **2** proceeds cleanly to give only *p*-nitrophenolate and nitrophenyl phosphate, as observed by thin-layer chromatography. Like **1**, **2** is selective for hydrolysis of diesters over monoesters; the rate of hydrolysis of BNPP is at least 500 times greater than the rate of hydrolysis of the monoester 4-nitrophenyl phosphate. Inhibition studies, shown in Figure 1, revealed that 4-nitrophenyl phosphate is a weak inhibitor in the hydrolysis of BNPP by **2**. A 10 equiv amount of 4-nitrophenyl phosphate slows the reaction to 50% of its uninhibited rate. The reaction is more strongly inhibited by inorganic pyrophosphate (PP<sub>i</sub>), being essentially shut down at only 1 equiv of PP<sub>i</sub> with respect to metal complex. These inhibition profiles parallel those of **1**. Other coordinating anions such as carbonate and EDTA also inhibit hydrolysis of BNPP by **2** at relatively low concentrations. A 1 equiv amount of carbonate completely shuts down the reaction, while 1 equiv of EDTA slows the reaction by 50% (data not shown). Ionic strength has a moderate effect on the catalytic efficiency of **2**, with a 10-fold increase in ionic strength resulting in a 30–40% decrease in the rate of BNPP hydrolysis at pH 7.1, and a 20% decrease in rate at pH 9.1.

**Determination of the Rate Law for Cu(*i*-Pr<sub>3</sub>9)aneN<sub>3</sub>)<sup>2+</sup>-Catalyzed BNPP Hydrolysis.** Metal- and substrate-dependence experiments were consistent with the rate law

$$\text{rate} = k_{1,5}[\mathbf{2}]^{1/2}[\text{BNPP}]$$

as had been demonstrated for **1**.<sup>21</sup> Substrate dependence, shown in Figure 2A, is first order. Half-order metal dependence was observed over a narrow range of concentrations at 50 °C. At concentrations of **2** greater than 0.6 mM, the reaction rate became too fast to measure accurately by the method of initial rates under the conditions employed, with 5% conversion of substrate occurring in less than 15 s. At concentrations of **2** below 0.1 mM, the order with respect to metal was indeterminate. This change in reaction order is not surprising; the metal dependence is expected to be quadratic, a parabola with an origin at (0,0).<sup>21</sup> Half-order

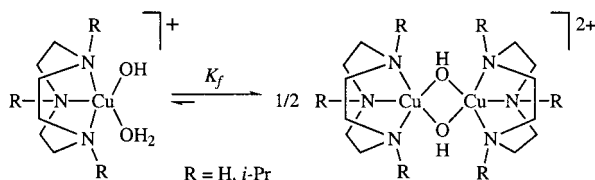


**Figure 2.** Concentration dependence of BNPP hydrolysis by **2**. Reactions were carried out at pH 9.2 in 50 mM CHES buffer, at an ionic strength of 0.10 M (adjusted with NaNO<sub>3</sub>). (a) Dependence of the rate on the concentration of BNPP (0.03 mM to 10 mM) at fixed [**2**] (0.17 mM) and 50 °C. (b) Dependence of the rate on the concentration of [**2**] (0.03–3.3 mM) at fixed [BNPP] (1.0 mM) and 35 °C. The line shown was fit to a subset of the data (0.2–3.3 mM **2**).

dependence is expected only when substantial amounts of dimer are present. In the limiting case of very low metal concentrations, first-order metal dependence is expected. At intermediate concentrations of metal complex, the order of reaction will be indeterminate, as is observed below 0.1 M **2** at 50 °C. To accurately measure the half-order rate constant, metal-dependence studies were performed at lower temperatures where a wider range of metal concentrations could be used. The half-order metal dependence from data obtained at 35 °C is shown in Figure 2B. Using the 1.5-order rate constant determined at three temperatures and extrapolating to 50 °C, a value of  $6.4 \times 10^{-2} \text{ M}^{-1/2} \text{ s}^{-1}$  was calculated for  $k_{1,5}$  at 50 °C. This extrapolated value agrees closely with the directly determined value ( $5.6 \times 10^{-2} \text{ M}^{-1/2} \text{ s}^{-1}$ ) obtained from a narrow range of metal concentrations at 50 °C. The 1.5-order rate constant for **2**-catalyzed BNPP hydrolysis is 2 orders of magnitude greater than the  $k_{1,5}$  of the parent catalyst ( $2.0 \times 10^{-4} \text{ M}^{-1/2} \text{ s}^{-1}$  at pH 9.2, 50 °C).<sup>26</sup>

The half-order metal dependence, shown previously for **1**,<sup>20,21</sup> Cu([10]aneN<sub>3</sub>)<sup>2+</sup>, and Cu([11]aneN<sub>3</sub>)<sup>2+</sup>,<sup>26</sup> is consistent with a monomer–dimer equilibrium (Scheme 1), where the monomer is the catalytically active species. The value of the dimer formation constant,  $K_f$ , for **2** was estimated from plots of the half-order metal dependence using the method of Deal et al.<sup>21,31</sup> Two limitations of this method for the present data are (1) the narrow range of concentrations of **2** that could be studied at 50 °C and (2) the assumption that  $2K_f[\text{Cu}]_{\text{T}} \gg 0.25$  (where  $[\text{Cu}]_{\text{T}}$  is the total copper complex

## Scheme 1

**Table 2.** Temperature Dependence of the Rate Constant for 2-Catalyzed BNPP Hydrolysis and the Dimer Formation Constant of 2<sup>a</sup>

temp (°C)	$k_{1.5}^b$ (M <sup>-1/2</sup> s <sup>-1</sup> )	$K_f^{b,c}$ (M <sup>-1</sup> )	$K_f^d$ (M <sup>-1</sup> )
15	0.0056	453	57
27	0.014	659	94
35	0.024	901	126
50	0.056	1353	
50 <sup>e</sup>	0.064	1394	216

<sup>a</sup> Reaction conditions at all temperatures were as follows: 1.0 mM BNPP, 50 mM CHES, pH 9.2, 0.10 M ionic strength (adjusted with NaNO<sub>3</sub>). <sup>b</sup> Concentration ranges of **2** giving linear half-order plots were 0.60–3.67 mM at 15 °C, 0.30–3.0 mM at 27 °C, 0.20–3.3 mM at 35 °C, and 0.12–0.60 mM at 50 °C. <sup>c</sup>  $K_f$  determined using the method of Deal et al.<sup>21</sup> <sup>d</sup>  $K_f$  determined using nonlinear fits of the metal dependence data over the following concentration ranges of **2**: 0.13–3.67 mM at 15 °C; 0.05–4.0 mM at 27 °C; 0.02–3.3 mM at 35 °C. <sup>e</sup> Values in this row are extrapolated from the data at 15, 27, and 35 °C.

concentration). To address the first limitation, the values of  $K_f$  were determined at various temperatures, shown in Table 2, and a plot of  $\ln K_f$  vs  $1/T$  was extrapolated to 50 °C. The extrapolated value at 50 °C (1394 M<sup>-1</sup>) agreed well with the experimentally determined value (1353 M<sup>-1</sup>) obtained over a limited concentration range. To address the second limitation, the assumption  $2K_f[\text{Cu}]_T \gg 0.25$ , the data at each temperature were fit to a nonlinear function, given in equation 1.

$$\text{rate} = k_{\text{obs}}(-1/2 + (1/4 + 2K_f[\text{Cu}]_T)^{1/2})/2K_f \quad (1)$$

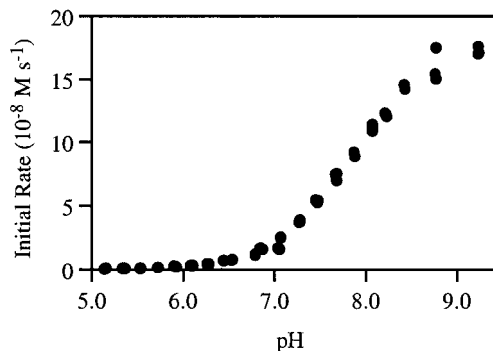
This equation eliminates the need for the assumption and allows for use of a wider range of metal concentrations at all temperatures, as it takes into account the intrinsic nonlinear dependence of the reaction rate on metal concentration. Because only a limited amount of data was available at 50 °C, the value of  $K_f$  at 50 °C was extrapolated from the calculated  $K_f$  values at the three lower temperatures. The values of  $K_f$  determined by both the method of Deal et al.<sup>21,31</sup> and the nonlinear curve fit method are presented in Table 2. The estimated value of  $K_f$  at 50 °C is in the range from 216 to 1394 M<sup>-1</sup>, which is at least an order of magnitude lower than the  $K_f$  for **1** and at most half as great as that for Cu([11]aneN<sub>3</sub>)<sup>2+</sup> (Table 3). A plot of  $\ln K_f$  vs  $1/T$  reveals a positive enthalpy of formation of the dimer of  $27 \pm 3$  kJ mol<sup>-1</sup>, revealing that dimerization of **2** is endothermic.<sup>32</sup>

The pH dependence of **2**-catalyzed BNPP hydrolysis, shown in Figure 3, is consistent with deprotonation of a coordinated water molecule to form the active catalyst. The rate of hydrolysis increases by 2 orders of magnitude in going

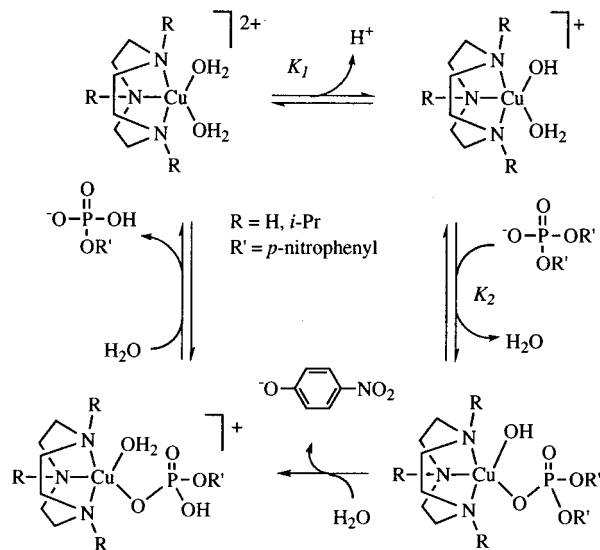
**Table 3.** Geometric Parameters, Measured pK<sub>a</sub>s, Dimer Formation Constants and 1.5-Order Rate Constants for a Series of BNPP Hydrolysis Catalysts

	cone angle <sup>a</sup> (deg)	pK <sub>a</sub> <sup>b</sup>	$K_f^c$ (M <sup>-1</sup> )	$k_{1.5}^c$ (M <sup>-1/2</sup> s <sup>-1</sup> )
<b>1</b>	102	7.3	13 000	$2.0 \times 10^{-4}$
Cu([10]aneN <sub>3</sub> )Br <sub>2</sub>	127	7.6	5 300	$4.0 \times 10^{-4}$
Cu([11]aneN <sub>3</sub> )Br <sub>2</sub>	118	8.2	2 700	$1.6 \times 10^{-3}$
<b>2</b>	208	8.7	1 400 <sup>d</sup>	$6.0 \times 10^{-2}$

<sup>a</sup> Cone angle analyses was performed using vector algebra applied to the xyz atomic coordinates from the published crystal structures of **1**,<sup>41</sup> Cu([10]aneN<sub>3</sub>)Br<sub>2</sub>,<sup>26</sup> Cu([11]aneN<sub>3</sub>)Br<sub>2</sub>,<sup>26</sup> and **2**.<sup>27</sup> <sup>b</sup> Measured at 25 °C and 0.10 M ionic strength; note that at 50 °C the measured pK<sub>a</sub> for **2** is 7.9. <sup>c</sup> Values were determined at pH 9.2. <sup>d</sup> Upper limit given: range is from 216 to 1394 M<sup>-1</sup> (this work). Data for compounds **1**, Cu([10]aneN<sub>3</sub>)Br<sub>2</sub>, and Cu([11]aneN<sub>3</sub>)Br<sub>2</sub> are taken from the literature.<sup>21,26</sup>

**Figure 3.** pH dependence of **2**-mediated BNPP hydrolysis. Reactions were run at 50 °C, 0.10 M ionic strength (adjusted with NaNO<sub>3</sub>). [2] was 0.20 mM, and [BNPP] was 0.60 mM. The buffers (50 mM) were MES (pH 5.1–6.4), HEPES (pH 6.5–7.1), HEPPSO (pH 6.8–8.2), and CHES (pH 8.4–9.2).

## Scheme 2



from pH 5.5 to pH 9.2. The kinetic pK<sub>a</sub> of  $7.8 \pm 0.2$  closely matches the measured thermodynamic pK<sub>a</sub> ( $7.9 \pm 0.1$ , a composite of several equilibria) as determined by potentiometric titration at 50 °C. Thus the active form of the catalyst is most likely to be [Cu(*i*-Pr<sub>3</sub>[9]aneN<sub>3</sub>)(OH)(OH<sub>2</sub>)]<sup>+</sup>, completely analogous to the active species in **1**-catalyzed BNPP hydrolysis. A mechanism consistent with the kinetic data is given in Scheme 2.

**Activation Parameters for BNPP Hydrolysis.** Determination of the 1.5-order rate constants for **2**-catalyzed BNPP

(31) Deal, K. A. The Mechanism of Macrocyclic Copper(II) Catalyzed Phosphate Diester Hydrolysis. Ph.D. Thesis, University of Wisconsin–Madison, Madison, WI, 1993.

(32) Segel, I. H. *Biochemical Calculations*; 2nd ed.; John Wiley & Sons: New York, 1976.

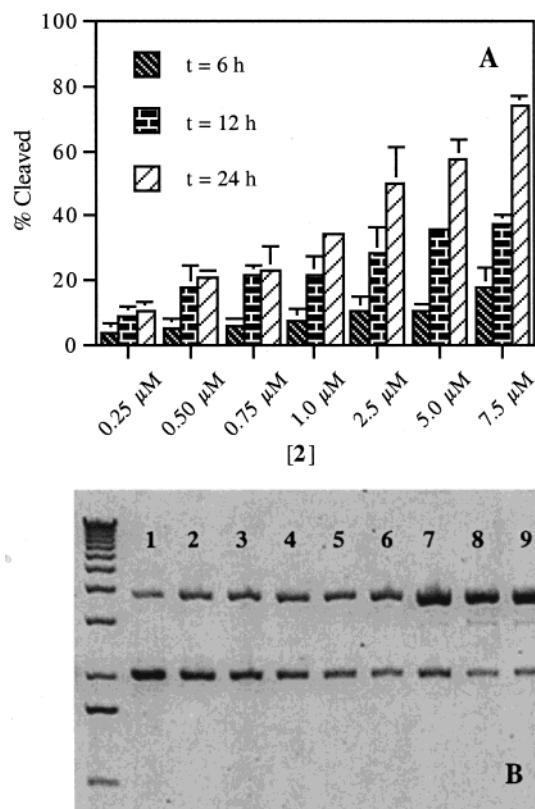


**Figure 4.** Cleavage of supercoiled plasmid pBluescript II KS(-) by **2**. (a) The reactions were carried out anaerobically with DNA (0.05 mg/mL) and **2** in HEPPSO (40 mM at pH 7.8) for 6, 12, and 24 h at 50 °C. The graph was created with the data from three separate experiments. The extent of cleavage was normalized to control reactions, and the error bars are standard deviations calculated using the formula for a small number of data points. Where error bars do not appear, the standard deviation is too small to appear on the bar graph. (b) A representative agarose gel showing plasmid pBluescript treated with various concentrations of **2** for 24 h at pH 7.8 and 50 °C. Lane 1: DNA control. Lane 2: DNA + 0.25  $\mu\text{M}$  **2**. Lane 3: DNA + 0.50  $\mu\text{M}$  **2**. Lane 4: DNA + 0.75  $\mu\text{M}$  **2**. Lane 5: DNA + 1.0  $\mu\text{M}$  **2**. Lane 6: DNA + 2.5  $\mu\text{M}$  **2**. Lane 7: DNA + 5.0  $\mu\text{M}$  **2**. Lane 8: DNA + 7.5  $\mu\text{M}$  **2**. Lane 9: DNA + 10  $\mu\text{M}$  **2**.

hydrolysis at four temperatures (Table 2) allowed us to calculate the activation parameters using the Arrhenius equation. The activation energy,  $E_a$ , was determined to be  $53 \pm 2$  kJ/mol. Using transition-state theory<sup>33,34</sup> we determined  $\Delta H^\ddagger$  to be  $51 \pm 2$  kJ/mol and  $\Delta S^\ddagger$  to be  $-110 \pm 6$  J/mol K. The activation enthalpy,  $\Delta H^\ddagger$ , is roughly half that for the parent complex, indicating a lower energy barrier to the transition state for **2**-catalyzed BNPP hydrolysis, while the activation entropies are roughly the same for the two catalysts, consistent with similarly organized transition states.

**Cleavage of Double-Stranded DNA.**  $\text{Cu}(i\text{-Pr}_3[9]\text{aneN}_3)^{2+}$  efficiently cleaves double-stranded supercoiled plasmid DNA at near-physiological pH under anaerobic conditions. Experiments to explore time and concentration dependence of **2**-mediated DNA cleavage were carried out at pH 7.8 and 50 °C. As shown in Figure 4, **2** cleaves plasmid DNA at sub-micromolar concentrations, and the cleavage exhibits

**Table 4.** Anaerobic Cleavage of Supercoiled pBluescript II ks(-) by **2**<sup>a</sup>

incubation time (h)	$[\text{Cu}(i\text{-Pr}_3[9]\text{aneN}_3)^{2+}]^a$ (mM)	DNA % form		
		supercoiled	nicked	linear
6	control	91 $\pm$ 5	9 $\pm$ 5	0 $\pm$ 0
	0.25	87 $\pm$ 7	13 $\pm$ 7	0 $\pm$ 0
	0.50	85 $\pm$ 7	15 $\pm$ 7	0 $\pm$ 0
	0.75	85 $\pm$ 7	15 $\pm$ 7	0 $\pm$ 0
	1.0	84 $\pm$ 6	16 $\pm$ 6	0 $\pm$ 0
	2.5	80 $\pm$ 9	20 $\pm$ 8	0 $\pm$ 0
	5.0	81 $\pm$ 5	19 $\pm$ 5	0 $\pm$ 0
	7.5	73 $\pm$ 10	27 $\pm$ 10	0 $\pm$ 0
12	control	90 $\pm$ 2	10 $\pm$ 2	0 $\pm$ 0
	0.25	81 $\pm$ 5	19 $\pm$ 5	0 $\pm$ 0
	0.50	71 $\pm$ 6	29 $\pm$ 6	0 $\pm$ 0
	0.75	68 $\pm$ 5	32 $\pm$ 5	0 $\pm$ 0
	1.0	67 $\pm$ 7	33 $\pm$ 7	0 $\pm$ 0
	2.5	61 $\pm$ 9	39 $\pm$ 9	0 $\pm$ 0
	5.0	54 $\pm$ 1	47 $\pm$ 1	0 $\pm$ 0
	7.5	52 $\pm$ 4	48 $\pm$ 4	0 $\pm$ 0
24	control	87 $\pm$ 2	13 $\pm$ 2	0 $\pm$ 0
	0.25	76 $\pm$ 3	24 $\pm$ 3	0 $\pm$ 0
	0.50	67 $\pm$ 2	33 $\pm$ 2	0 $\pm$ 0
	0.75	65 $\pm$ 6	34 $\pm$ 7	1 $\pm$ 1
	1.0	54 $\pm$ 2	45 $\pm$ 2	1 $\pm$ 1
	2.5	39 $\pm$ 12	59 $\pm$ 10	2 $\pm$ 2
	5.0	33 $\pm$ 1	64 $\pm$ 2	3 $\pm$ 3
	7.5	18 $\pm$ 6	79 $\pm$ 5	3 $\pm$ 1

<sup>a</sup> The reactions were carried out under inert atmosphere with plasmid DNA (150  $\mu\text{M}$  bp), and **2** at the specified concentrations in HEPPSO (40 mM at pH 7.8) for 6, 12, and 24 h at 50 °C. This table was created with the data from at least three separate experiments, and the errors are standard deviations calculated using the formula for a small number of data points.

both time and metal complex concentration dependence. Treatment of plasmid DNA with **2** for up to 12 h resulted in conversion of supercoiled (form I) DNA to nicked (form II) DNA. After treatment with **2** for 24 h, linear (form III) DNA is also observed (Table 4).

Since the efficiency of BNPP hydrolysis by **2** varies with pH, the effect of pH on DNA cleavage was explored. The reaction pH range was selected to span the region of maximal sensitivity to pH (i.e., maximal slope) in the pH dependence study of **2**-catalyzed BNPP hydrolysis (Figure 3). DNA cleavage was performed at pH 7.2 and 7.8; **2** is approximately 2-fold more efficient at cleaving DNA at the higher pH (Figure 5). This trend of increasing DNA cleavage efficiency with increasing pH is consistent with the requirement for deprotonation of a Cu-coordinated water in the DNA cleavage reaction.

**Comparison of the DNA Cleavage Efficiencies of  $\text{Cu}(i\text{-Pr}_3[9]\text{aneN}_3)^{2+}$  and  $\text{Cu}([9]\text{aneN}_3)^{2+}$ .** The exploration of the concentration dependence of plasmid DNA cleavage confirmed that **2** is a substantially more efficient DNA cleavage agent than **1**. To determine the optimal conditions for degradation of plasmid DNA by **2**, concentration dependence was studied over a range of 3 orders of magnitude (Figure 6). Interestingly, the amount of DNA cleavage is proportional to the increasing concentration of **2** up to 10  $\mu\text{M}$ , after which the amount of DNA cleavage decreases as the concentration of **2** increases. Such a trend was not observed in our original study of DNA cleavage by **1**.<sup>23</sup> To accurately compare the DNA cleavage efficiency of **2** with that of **1**, DNA cleavage activity of **1** was also studied over a similar range of concentrations. The concentration dependence for degrada-

(33) Bunnett, J. F. In *Investigation of Rates and Mechanisms of Reactions*; 4th ed.; Claude, F., Berasconi, E., Eds.; John Wiley & Sons: New York, 1986; Vol. 1.

(34) Jordan, R. B. *Reaction Mechanisms of Inorganic and Organometallic Systems*; 2nd ed.; Oxford University Press: New York, 1998.

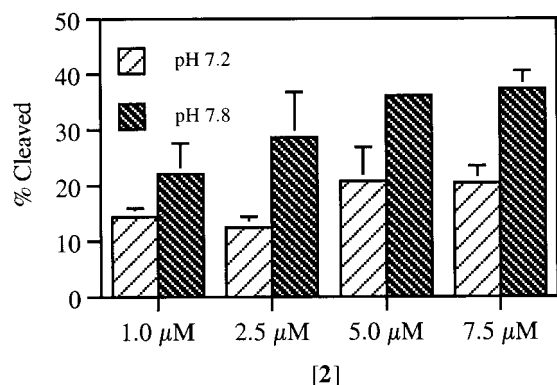


**Figure 5.** Extent of anaerobic cleavage of supercoiled plasmid DNA by **2** at pH 7.2 and pH 7.8. The reactions were carried as described in Figure 4 in HEPPSO (40 mM at pH 7.2 and 7.8) for 12 h at 50 °C. This graph was created with data from three separate experiments, and the error bars are standard deviations calculated using the formula for a small number of data points. Where error bars do not appear, the standard deviation was too small to appear on the bar graph. The extent of cleavage was normalized to control reactions.

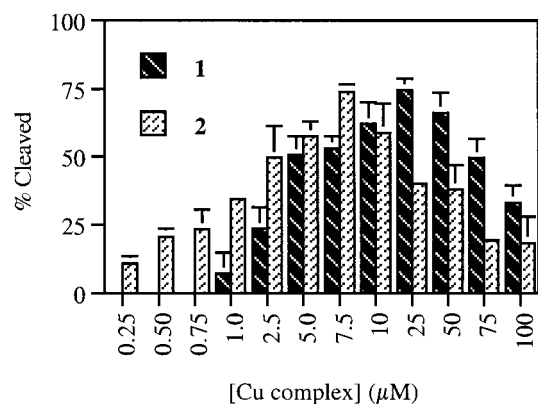


**Figure 6.** Direct comparison of anaerobic cleavage of supercoiled plasmid DNA by **2** and **1**. The reactions were carried out as described in Figure 4 for 24 h at 50 °C. This graph was created with data from three separate experiments, and the error bars are standard deviations calculated by using the formula for a small number of data points. Where error bars do not appear, the standard deviation was too small to appear on the bar graph.

tion of plasmid DNA by **1** follows a pattern similar to that of **2**; from 1.0 to 25 μM **1**, the amount of DNA cleavage is proportional to the increasing concentration of metal complex. At concentrations higher than 25 μM **1**, the relationship reverses; increasing concentrations of **1** decrease the amount of DNA cleaved. In comparing the two copper complexes, the concentration of **1** necessary to cleave 75% of the supercoiled plasmid DNA is 2.5 times higher than the concentration of **2** necessary to achieve the same extent of cleavage.

## Discussion

Compound **2** is a significantly more efficient phosphodiester hydrolysis catalyst and DNA cleavage agent than the related complex **1** previously reported. Dimer formation, which was a major limiting factor in the efficiency of BNPP hydrolysis by **1**, has been largely overcome by the presence of bulky substituents on the macrocycle in **2**. Significantly, the substantial rate enhancement for **2**-catalyzed BNPP hydrolysis exceeds that expected solely on the basis of the

decrease in magnitude of the dimer formation equilibrium constant,  $K_f$ . The greatly increased efficiency of **2** compared to **1** is due to a lower barrier to the transition state. DNA cleavage studies comparing the two complexes reveal that lower concentrations of **2** than **1** effect DNA cleavage.

**Mechanism of BNPP Hydrolysis.** As shown in Table 3, the equilibrium constant ( $K_f$ ) for formation of the bis-( $\mu$ -hydroxide) bridged dimer (Scheme 1) is substantially lower for **2** than it is for the other copper(II) macrocycles we have studied, consistent with increased steric demand of the ligand in **2**. An appropriate metric of steric bulk in metal complexes is the cone angle;<sup>35,36</sup> we have defined the cone angle as the included angle of the cone formed by the metal (vertex) and three non-hydrogen ligand atoms, either the nitrogens (for the nonalkylated rings) or the methine carbons (for the alkylated macrocycle in **2**). The crystallographic atom centers, not the van der Waals radii, have been used to define the points on the cone. As shown in Table 3, the steric bulk of the ligand in **2**, which has a cone angle greater than 180°, greatly exceeds the steric bulk of the ligands in the [9]–[11] series, which all have cone angles well below 180°. In the prior structure–reactivity studies, steric requirements of the ligands were compared on the basis of the sum of the three N–Cu–N angles.<sup>26</sup> While the angle sum is an appropriate metric when considering ring size of the macrocycle, this sum is not as useful when bulky substituents are introduced onto the ring. The formation of a bis-( $\mu$ -hydroxide) dimer of **2** is not expected to be energetically favorable due to steric interactions between the isopropyl groups, although the rings on the copper can be staggered with respect to one another so that the isopropyl groups interdigitate. Indeed, the temperature dependence of  $K_f$  (Table 2) reveals dimer formation to be endothermic for **2**.

The decrease in the dimer formation constant only partially accounts for the rate increase in the hydrolysis of BNPP by **2**. Using the values of  $K_f$  at pH 9.2, a simple calculation derived from the kinetic equations<sup>21,31,37</sup> allows one to estimate the relative amounts of inactive dimer and active monomer for both **1** and **2**. The estimated concentration of active monomer is only about two to three times as great for **2** as it is for **1**; yet the BNPP hydrolysis rate increased 60–70 times in a direct comparison of the two catalysts, and the 1.5-order rate constant for BNPP hydrolysis is 2 orders of magnitude greater for **2** than for **1**. These observations led us to explore other possible contributors to the significant rate enhancement.

Electronic characteristics of the catalysts, including Lewis acidity, hydrophobicity, and hydrogen bonding ability, were considered, but no significant contributions to the trend in hydrolytic efficiency could be discerned. Lewis acid activation of the substrate is generally thought to play an important role in the efficacy of chemical nucleases.<sup>38,39</sup> The measured  $pK_a$  of coordinated water in complexes is one indicator of

(35) Brown, T. L.; Lee, K. J. *Coord. Chem. Rev.* **1993**, *128*, 89–116.

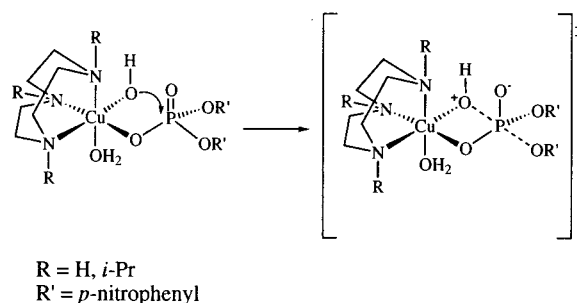
(36) Mueller, T. E.; Mingos, D. M. P. *Transition Met. Chem.* **1995**, *20*, 533–539.

(37) Original equation has the assumption  $2K_f[Cu]_{total} \gg 0.25$ . Here we use the full equation without the assumption; thus,  $[monomer] = (-1/2 + (1/4 + 2K_f[Cu]_{total})^{1/2})/2K_f$ .

Lewis acidity; on this basis **2** is the *least* acidic of the group including **1**,  $\text{Cu}([\text{10}] \text{aneN}_3)^{2+}$ ,  $\text{Cu}([\text{11}] \text{aneN}_3)^{2+}$ , and **2**, yet **2** is the *most* hydrolytically active (Table 3). Even at a pH below its apparent  $\text{pK}_a$ , **2** is 70 times more rapid at hydrolyzing BNPP than is **1** (Table 1). It appears that the properties of the complexes reflected in the measured  $\text{pK}_a$  values do not account for the trend in hydrolytic efficiency. If, however, one considers only the rate-determining step, i.e., loss of the leaving group,<sup>22</sup> it might be expected that a weaker Lewis acid would more easily release the negatively charged *p*-nitrophenolate product. The differing hydrophobicity of the ligand may also contribute to the greater efficiency of **2** as a catalyst. The alkylated ligand, *i*-Pr<sub>3</sub>[9]-aneN<sub>3</sub>, provides a more hydrophobic environment than [9]-aneN<sub>3</sub>, favoring binding of the substrate at low pH where the BNPP is largely in an uncharged, protonated state. At higher pH (e.g., 9.2), however, it would be expected that the electrostatic attraction of deprotonated, negatively charged BNPP to the positively charged metal complex would dominate, and consequently hydrophobic effects would be less important. Finally, whereas [9]aneN<sub>3</sub>, [10]aneN<sub>3</sub>, and [11]aneN<sub>3</sub> ligands can participate in hydrogen bonding with solvent water molecules, the *i*-Pr<sub>3</sub>[9]ane ligand does not have a proton on the nitrogen and thus cannot participate in such interactions. Hydrogen bonding, in which the N–H of the ligand serves as a hydrogen bond donor to a solvent water molecule, would be expected to create partial negative charge on the ligand nitrogen atoms. This charge effect would make the ligand a better  $\sigma$  donor to the metal and raise the  $\text{pK}_a$  of coordinated water. However, the measured  $\text{pK}_a$  of **1** is lower than the measured  $\text{pK}_a$  of **2**, inconsistent with the predicted trend based on this simple H-bonding model.

The lowered barrier to the transition state for BNPP hydrolysis by **2** is a significant contributor to the efficacy of **2** as a catalyst. The  $\Delta H^\ddagger$  for **2**-catalyzed BNPP hydrolysis is  $51 \text{ kJ mol}^{-1}$  (pH 9.2), while the  $\Delta H^\ddagger$  for **1**-catalyzed BNPP hydrolysis is  $90 \text{ kJ mol}^{-1}$  (pH 9.0).<sup>21</sup> The lowering of this barrier by the catalyst **2** could come about either by a stabilization of the transition state for **2** relative to **1** or by a destabilization of the catalyst–substrate complex (the species preceding the transition state) for **2**. The concerted transition-state consistent with isotope effect studies for **1**-catalyzed BNPP hydrolysis is shown in Scheme 3.<sup>22,40</sup> It is reasonable to propose the same transition state for **2**-catalyzed BNPP hydrolysis as for **1**-catalyzed BNPP hydrolysis, because the coordination geometry at the copper center is similar for the two complexes. In the solid-state both **1** and **2** exhibit distorted square pyramidal geometry.<sup>27,41</sup> While the sum of the N–Cu–N angles is slightly larger for **2** ( $262^\circ$ ) than for **1** ( $248^\circ$ ), the Cu–N distances in the two complexes are very similar. Assuming **2** does employ the same transition state as **1**, there is an important difference that becomes apparent

Scheme 3



when examining molecular models. The phenyl rings of the bound substrate can interact with the isopropyl groups on the macrocycle in **2**; therefore, it seems unlikely that this transition-state structure would be stabilized by the bulky *i*-Pr<sub>3</sub>[9]aneN<sub>3</sub> ligand. We propose instead that both the transition state and the catalyst–substrate complex preceding it are *destabilized* in **2**- relative to **1**-catalyzed BNPP hydrolysis. To be consistent with our observations, the catalyst–substrate complex for **2** must be destabilized to a greater extent than its transition state. Such a destabilization places the catalyst–substrate complex, formed by fast ligand exchange, closer in energy to the transition state for **2** than for **1**, thereby increasing the rate of BNPP hydrolysis.

**Cleavage of DNA.** Cleavage of DNA was performed under anaerobic conditions to eliminate oxidative chemistry and to prevent exposure to CO<sub>2</sub>, which can result in the formation of a carbonate complex. Previously, we observed at least two different mechanisms for the degradation of DNA using **1**:<sup>23</sup> an O<sub>2</sub>-dependent pathway and an O<sub>2</sub>-independent pathway. For the purposes of this study, we are more interested in the potentially hydrolytic, O<sub>2</sub>-independent pathway. Over extended time periods, the hydrolytic activity of **2** is sensitive to carbonate ions, which may enter the reaction solution by exposure to CO<sub>2</sub> from the atmosphere at moderately elevated pH. On extended incubation at above neutral pH, complex **2** reacts with carbonate to form an insoluble material, possibly a carbonate bridged dimer that has been structurally characterized.<sup>42</sup> While exposure to CO<sub>2</sub> was not a concern in studying BNPP hydrolysis where the reactions are monitored for short time periods in sealed cells with minimal headspace, exposure to CO<sub>2</sub> becomes a concern in studying DNA cleavage because the reactions are carried out for 24 h.

Complex **2** effectively cleaves DNA under anaerobic conditions, and the pH and concentration dependence of DNA cleavage is suggestive of a mechanism similar to that observed for BNPP hydrolysis. Cleavage of double-stranded DNA by **2** is both time and concentration dependent, consistent with the conclusion that the metal complex is effecting DNA scission. Moreover, **2** cleaves DNA at very low concentrations, significantly lower than the concentrations of **1** that we previously used to cleave DNA. This observation led us to reexamine the concentration dependence of **1**-promoted DNA cleavage for comparison. DNA cleavage

(38) Wall, M.; Hynes, R. C.; Chin, J. *Angew. Chem., Int. Ed. Engl.* **1993**, *32*, 1633–1635.

(39) Williams, N. H.; Chin, J. *Chem. Commun.* **1996**, 131–132.

(40) Kavana, M.; Powell, D. R.; Burstyn, J. N. *Inorg. Chim. Acta* **2000**, *297*, 351–361.

(41) Schwindinger, W. F.; Fawcett, T. G.; Lalancette, R. A.; Potenza, J. A.; Schugar, H. J. *Inorg. Chem.* **1980**, *19*, 1379–1381.

(42) Schneider, J. L.; Young, V. G., Jr.; Tolman, W. B. *Inorg. Chem.* **1996**, *35*, 5410–5411.

by both **2** and **1** increases as the concentration of the metal complex increases up to a maximal effective concentration. As the concentration of metal complex is increased further, the extent of DNA cleavage decreases with further increases in metal complex concentration. A plausible explanation for this effect, assuming a mechanism similar to that observed for BNPP hydrolysis, is an increase in concentration of the inactive hydroxide bridged dimers as the concentration of metal ion increases. The dimers of the **1** and **2** might inhibit DNA cleavage by blocking access of the active monomers to the DNA backbone. Electrostatic considerations suggest that the dimers should interact more strongly with DNA than the monomers due to an increase in positive charge. The more highly charged dimeric species may effectively compete for binding to the negatively charged DNA backbone, but be unable to effect DNA cleavage. Contrary to these arguments, the effectiveness of the two complexes correlates inversely with the magnitude of the dimer formation constants and therefore does not correlate with the predicted concentrations of dimeric species. The greater effectiveness of **2** for DNA cleavage at low concentrations does correlate with the greater effectiveness of this catalyst in BNPP hydrolysis. It is plausible that similar mechanisms are operative in DNA cleavage and BNPP hydrolysis and that

the more efficient DNA cleavage observed with **2** is again due to a lowering of the barrier to the transition state.

## Conclusions

We have demonstrated that **2** efficiently hydrolyzes an activated phosphodiester and cleaves double-stranded DNA. The mechanism for hydrolysis of BNPP by **2** appears to be the same as that reported for **1**, Cu([10]aneN<sub>3</sub>)<sup>2+</sup>, and Cu([11]aneN<sub>3</sub>)<sup>2+</sup>. The increased efficiency of **2** compared to the other catalysts in the family is not accounted for only by the decrease in  $K_f$ ; energetic factors are also important. We have also shown that, under anaerobic conditions, both **1** and **2** cleave DNA at micromolar concentrations of metal complex and near physiological pH, but **2** is effective at lower concentrations than **1**.

**Acknowledgment.** The authors thank Dr. Francis J. Deck for cone angle analysis and nonlinear fits of metal concentration and pH dependence data. T.A.T. acknowledges support from the Chemistry-Biology Interface Training Grant, GM-08505. Support of the Wisconsin Alumni Research Foundation through the Technology Innovation Fund is gratefully acknowledged.

IC0107025